Hindawi Publishing Corporation
Journal of Nanomaterials
Volume 2012, Article ID 814915, 10 pages
doi:10.1155/2012/814915

Research Article

Consolidation of Amorphous $Al_{80}Fe_{10}Ti_5Ni_5$ Powders by Hot Pressing

M. Tavoosi,[1,2] F. Karimzadeh,[1] M. H. Enayati,[1] and H. S. Kim[2]

[1] *Department of Material Engineering, Nanotechnology and Advanced Material Institute, Isfahan University of Technology (IUT), Isfahan 84156-83111, Iran*
[2] *Department of Materials Science and Engineering, Pohang University of Science and Technology (POSTECH), Pohang 790-784, Republic of Korea*

Correspondence should be addressed to H. S. Kim, hskim@postech.ac.kr

Received 13 May 2012; Accepted 8 July 2012

Academic Editor: Mohammad H. Maneshian

The current study investigates the feasibility of fabricating amorphous $Al_{80}Fe_{10}Ti_5Ni_5$ powders by mechanical alloying and consolidating them into bulk samples by a hot-pressing technique. As-milled and hot-pressed samples were examined by X-ray diffraction, scanning electron microscopy, transition electron microscopy, and differential scanning calorimetry. The results showed that milling of $Al_{80}Fe_{10}Ti_5Ni_5$ powder for 40 h and hot pressing at 550°C under 600 MPa led to a fully dense bulk sample. During consolidation, an AlTi intermetallic phase with average crystallite size of 10 nm precipitates in the amorphous matrix.

1. Introduction

Alloys with Al content of 80 to 90 at.% have attracted considerable attention due to their combination of good ductility and high strength [1–7]. Among the various aluminum alloys, Al-Fe systems are of technological interest due to their advantageous properties, including high specific strength, high specific stiffness, good strength at intermediate temperatures, and excellent corrosion resistance at elevated temperatures under oxidizing, carburizing, and sulfidizing atmospheres [8–12]. A new class of Al-based alloys, which has received a great deal of attention in recent years, is amorphous as well as nanocrystalline [13–23].

Indeed, amorphous alloys exhibit several superior properties that cannot be obtained in crystalline materials. In general, bulk amorphous alloys can be fabricated by two main processes: direct solidification from the melt and consolidation of an amorphous powder or ribbons. Generally, very high cooling rates are required for the formation of an amorphous phase from the liquid state and only a few amorphous alloys with high glass-forming ability can be applied to the fabrication of bulk amorphous alloys by a direct solidification process. Due to the requirement of a high cooling rate, amorphous alloys have largely been fabricated in the form of powders, ribbons, and wires with small thickness or diameter [14–17], and hence the application of amorphous alloys as a structural material has been limited.

The glass-forming ability of Al-based alloys is so low and there is not any report about formation of bulk amorphous structure for these alloys by the use of direct solidification methods [11–13]. Nevertheless, a great number of amorphous alloys in Al-based alloys have been synthesized by various preparation methods of rapid quenching from liquid or vapor and solid-state reactions [13]. However, the maximum thicknesses of the resulting amorphous alloys have usually been limited. The limitation of the maximum sample thickness has prevented a wide extension of application fields of amorphous alloys. Consequently, great efforts have been devoted to preparation of a bulk amorphous alloy from amorphous alloy powder by using various techniques of warm pressing, warm extrusion, explosive compaction, hot pressing, and spark plasma sintering [13, 24]. The powder metallurgy process promotes high strength bonding between particles and a microstructure similar to that of a wrought product [25–30].

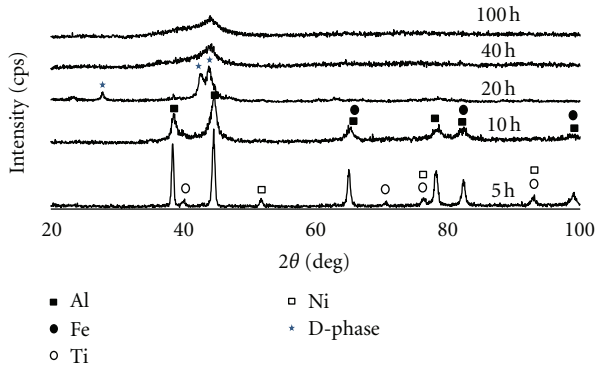

Figure 1: XRD patterns of the Al-10%Fe-5%Ni-5%Ti powder mixture after various milling times.

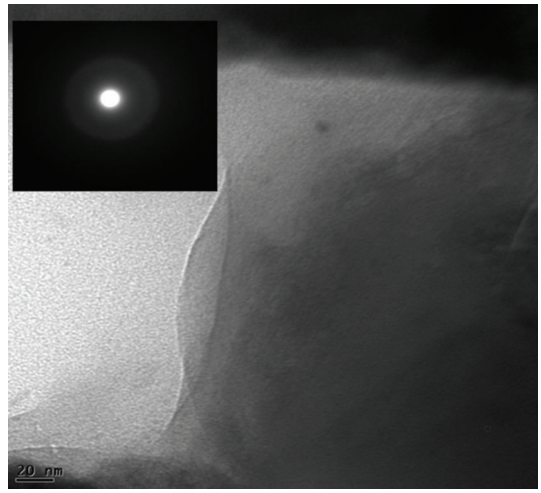

Figure 2: TEM image of the Al-10%Fe-5%Ti-5%Ni powder mixture after 40 h of MA.

The purpose of this study is the investigation of the feasibility of fabricating amorphous $Al_{80}Fe_{10}Ti_5Ni_5$ powders by mechanical alloying and consolidating them into bulk samples by a hot-pressing technique.

2. Experimental Procedure

Commercial elemental powders of Al (99%), Fe (99.9%), Ti (99%), and Ni (99.99%) were used as raw materials. The mixture of elemental powders with a composition of $Al_{80}Fe_{10}Ti_5Ni_5$ (in atomic percentage) was mechanically alloyed in a planetary ball mill under an argon atmosphere in a steel container at room temperature. A rotation speed of 250 rpm and a ball to powder ratio of 10 : 1 were employed. 1 wt% stearic acid powder supplied by Merck was used as the process control agent (PCA).

The produced amorphous powders were consolidated in a vacuum hot-pressing machine to prepare bulk amorphous discs with 10 mm diameter and 1 mm thickness. Hot pressing was performed at different temperatures and pressures. The hot-pressing chamber was evacuated and pressure was applied during the entire consolidating process.

The as-milled powders and consolidated samples were characterized by X-ray diffraction (XRD) analysis, scanning electron microscopy (SEM), transition electron microscopy (TEM), and differential scanning calorimetry. The XRD analysis was performed using a Philips diffractometer (40 kV) with Cu Kα radiation (λ = 0.15406 nm). The XRD patterns were recorded in the 2θ range of 30–70° (step size 0.03° and time per step 1 s). The morphology, fracture surface, and cross-sections of prepared samples were examined using SEM. The microstructure of the produced amorphous powder was investigated by TEM and a selected area diffraction (SAD) pattern analysis carried out at an accelerating voltage of 200 kV resolution of 0.19 nm. A differential thermal analysis (DTA) was conducted to study the thermal stability of the produced amorphous alloy using a Reometric STA 1500 differential thermal analyzer. The samples were placed in Al_2O_3 pans and heated in a dynamic Ar atmosphere up to 1200°C at a constant heating rate of 40°C/min.

3. Results and Discussion

3.1. Production of $Al_{80}Fe_{10}Ti_5Ni_5$ Amorphous Phase. The XRD patterns of the Al-10%Fe-5%Ni-5%Ti powder mixture after various milling times are shown in Figure 1. In the early stage of milling, broadening of Al, Fe, Ni, and Ti peaks

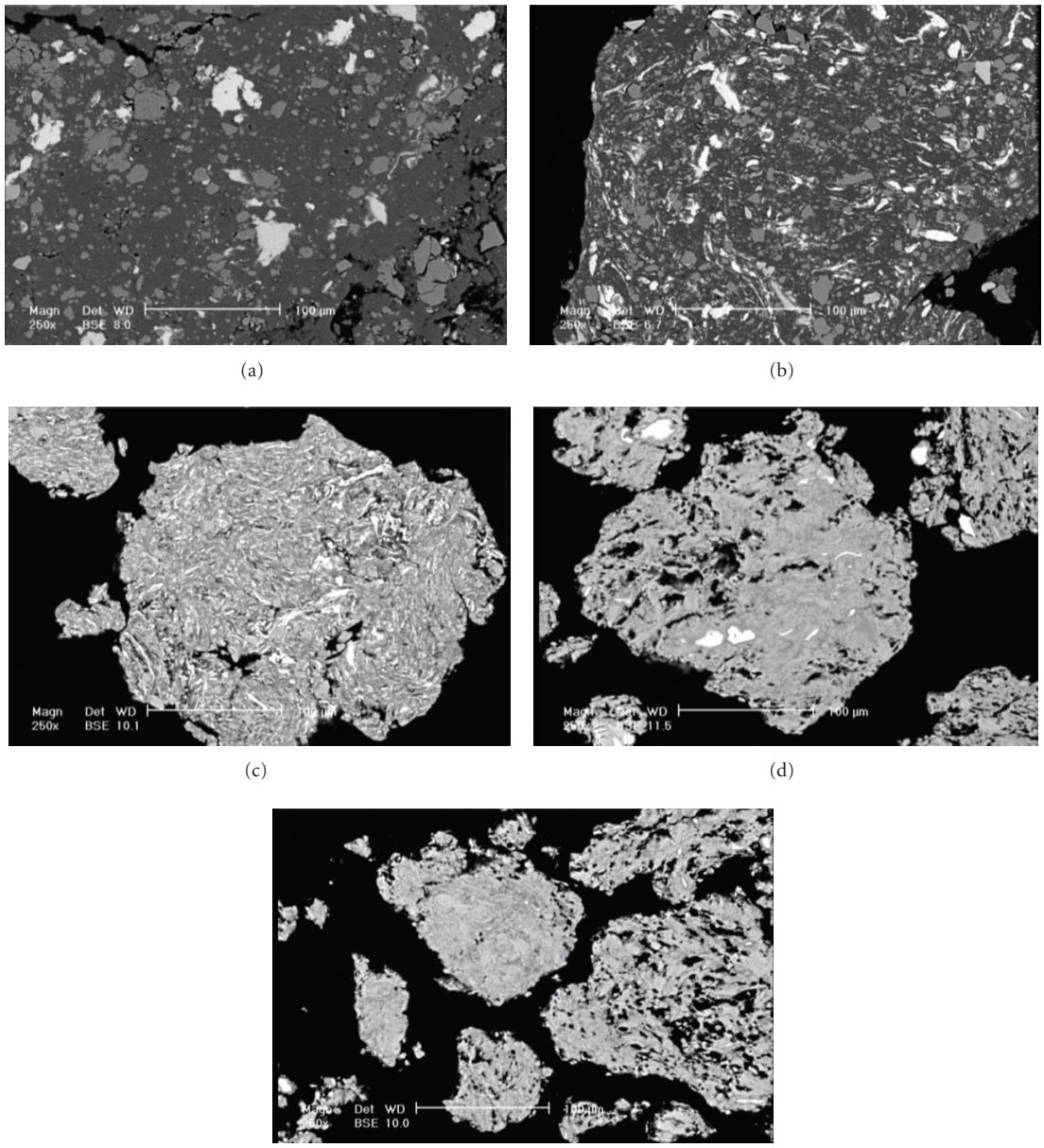

Figure 3: SEM cross-sectional micrographs of Al-10%Fe-5%Ti-5%Ni powder mixture after different milling times: (a) 0.25 h, (b) 0.5 h, (c) 1 h, (d) 5 h, and (e) 10 h.

accompanied by a remarkable decrease in their intensities occurred as a result of refinement of crystallite size and enhancement of lattice strain. Increasing milling time up to 10 h led to the disappearance of Fe, Ti, and Ni peaks. This may be due to dissolution of these elements in the Al lattice. By increasing the milling time, two narrow peaks corresponding to the decagonal phase (D-phase) are observed in the XRD patterns. Analysis of the XRD patterns in Figure 1 reveals that the D-phase, which formed from the solid solution during milling, could be amorphized by further milling (after 40 h) and there is no significant change as the milling time is prolonged to 100 h. A TEM micrograph and SAD pattern of powders ball milled for 40 h are also presented in Figure 2. As can be seen in this figure, the SAD pattern of this sample consists of only amorphous halo and there is no evidence of the presence of any crystalline phase, which is in agreement with the XRD result. This indicates that the product of mechanical alloying of the Al-10%Fe-5%Ni-5%Ti powder mixture is an amorphous phase.

SEM cross-sectional micrographs of powder particles after different milling times are presented in Figure 3. According to the micrographs, in the early stages of mechanical alloying (MA), the ductile components are flattened to platelet shapes, cold welded together, and form a composite

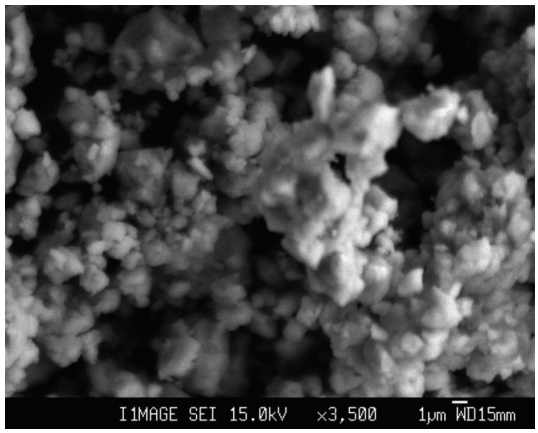

Figure 4: Morphology of Al-10%Fe-5%Ti-5%Ni powder mixture after 40 h of ball milling.

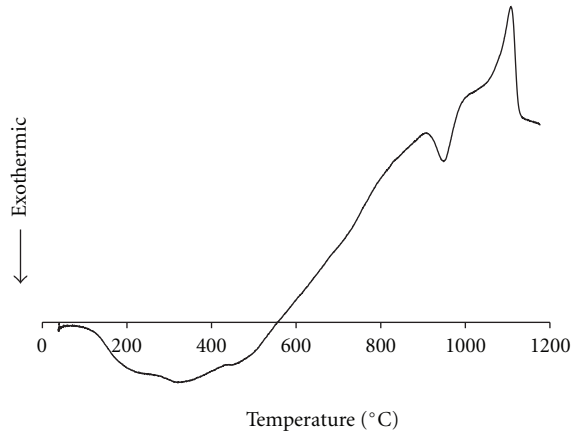

Figure 5: DSC curves of amorphous $Al_{80}Fe_{10}Ti_5Ni_5$ alloy at a constant heating rate of 40°C/min.

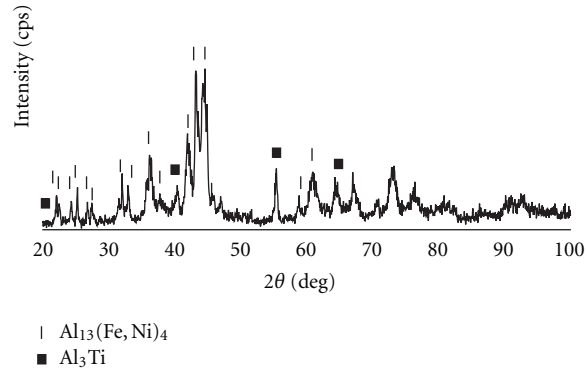

Figure 6: XRD pattern of amorphous $Al_{80}Fe_{10}Ti_5Ni_5$ alloy after isothermal annealing at 1000°C for 20 min.

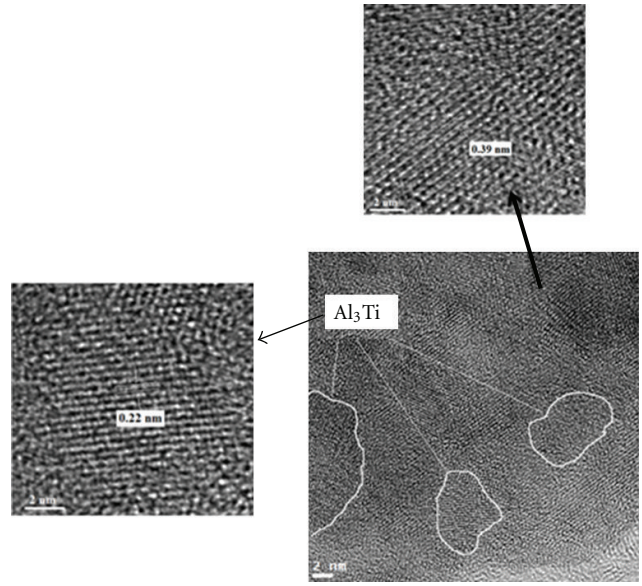

Figure 7: HRTEM image of amorphous $Al_{80}Fe_{10}Ti_5Ni_5$ alloy after isothermal annealing at 1000°C for 20 min.

lamellar structure of the constituent metals (Figures 3(a) and 3(b)). With increasing MA time, the composite powder particles are work hardened and fragmented. With further milling (Figures 3(c) and 3(d)), the interlamellar spacing decreases and true alloying at the atomic level occurs, resulting in the formation of solid solutions, intermetallics, or even amorphous phases. In this stage, the interlayer spacing disappears or becomes so fine that it is no longer visible using SEM (Figure 3(e)). The morphology of $Al_{80}Fe_{10}Ti_5Ni_5$ powders after 40 h of ball milling is also shown in Figure 4. As seen here, the powders milled for 40 h are spherical and have an average diameter of 2 μm.

3.2. Thermal Behavior of Produced Amorphous Powder. As noted in the previous section, milling the mixed powder for 40 h led to the formation of the $Al_{80}Fe_{10}Ti_5Ni_5$ amorphous phase. The mechanically milled microstructure is in a metastable state and considerable microstructural changes can occur upon heating the milled powder. In order to study the thermal stability of the produced amorphous phase, the sample was examined by DSC under continuous heating conditions. Figure 5 shows the DSC heating traces of the $Al_{80}Fe_{10}Ti_5Ni_5$ amorphous alloy at a constant heating rate of 20°C/min. As seen in this figure, two peaks appear in the DSC curve (an exothermic peak at 950°C and an endothermic peak at 1100°C). To analyze the crystallization process responsible for the exothermic peak, the as-blended sample was annealed under an Ar atmosphere at 1000°C for 20 min. The XRD pattern and a TEM micrograph of the $Al_{80}Fe_{10}Ti_5Ni_5$ amorphous phase after annealing at 1000°C are presented in Figures 6 and 7, respectively. As can be seen here, the annealed sample consists mainly of an $Al_{13}(Fe,Ni)_4$ [31] and Al_3Ti [32] intermetallic phases. Therefore, the exothermic peak in Figure 5 is attributed to precipitation of these phases from the amorphous phase. Meanwhile,

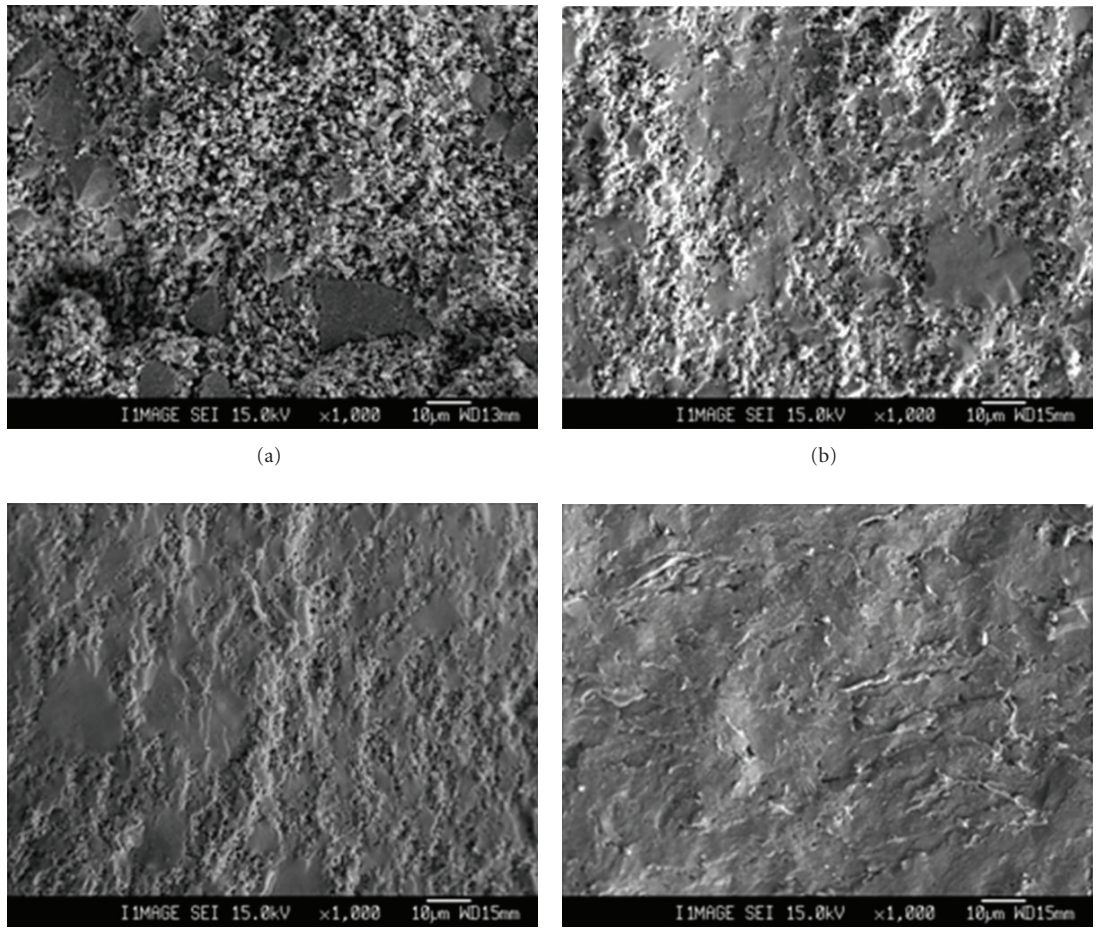

(a) (b)

(c) (d)

Figure 8: Fracture surface photographs of samples hot pressed at (a) 400°C, (b) 450°C, (c) 500°C, and (d) 550°C under a constant pressure 600 MPa.

the endothermic peak at 1100°C in Figure 5 is for the melting of the produced alloy. These results indicate that the total transformation sequence of the $Al_{80}Fe_{10}Ti_5Ni_5$ amorphous alloy is a one-stage process in the temperature range from 930°C to 980°C.

In fact, according to the DSC results, the crystallization in $Al_{80}Fe_{10}Ti_5Ni_5$ proceeds in the same manner as in the $Al_{80}Fe_{10}Ti_{10}$ [11] system and is different from that in $Al_{80}Fe_{20}$ [23] and $Al_{83}Fe_{17}$ [10] amorphous systems. In contrast to the $Al_{80}Fe_{10}Ti_5Ni_5$ amorphous alloy (which exhibits one-stage crystallization on heating), the $Al_{80}Fe_{20}$ and $Al_{83}Fe_{17}$ amorphous phases exhibit three-stage crystallization during heating.

3.3. Consolidation of the Ball-Milled Amorphous Powders. Fully amorphous powder particles with high crystallization temperature (950°C) in $Al_{80}Fe_{10}Ti_5Ni_5$ alloy provide good conditions for the fabrication of a bulk amorphous material. In this study, the as-milled powders were consolidated by hot pressing into a disk shape. To optimize the condensation parameter, the ball-milled amorphous powders were hot pressed at different temperatures (400, 450, 500, and 550°C) under various pressures (200, 300, 400, 500, and 600 MPa) for 30 min. In order to investigate the condensed samples, the fracture surface morphology after compression tests was examined using SEM. Fracture surface photographs of samples hot pressed at different temperatures under a constant pressure of 600 MPa and under different pressure values at a constant temperature of 550°C are shown in Figures 8 and 9, respectively. As seen in these figures, the trace of the interparticle boundaries between the powders increases and the porosity in the hot pressed samples decreases as the pressing temperature and pressure increase. These results indicate that the optimum temperature and pressure for consolidation of the amorphous powders via the hot-pressing method are 550°C and 600 MPa, respectively, in our experimental conditions. The polished cross-sectional view of the consolidated sample at 550°C under 600 MPa in Figure 10 shows no remaining pores.

Figure 11 shows the XRD pattern of the consolidated at 550°C under 600 MPa. From the peaks corresponding to AlTi, it can be concluded that the amorphous phase

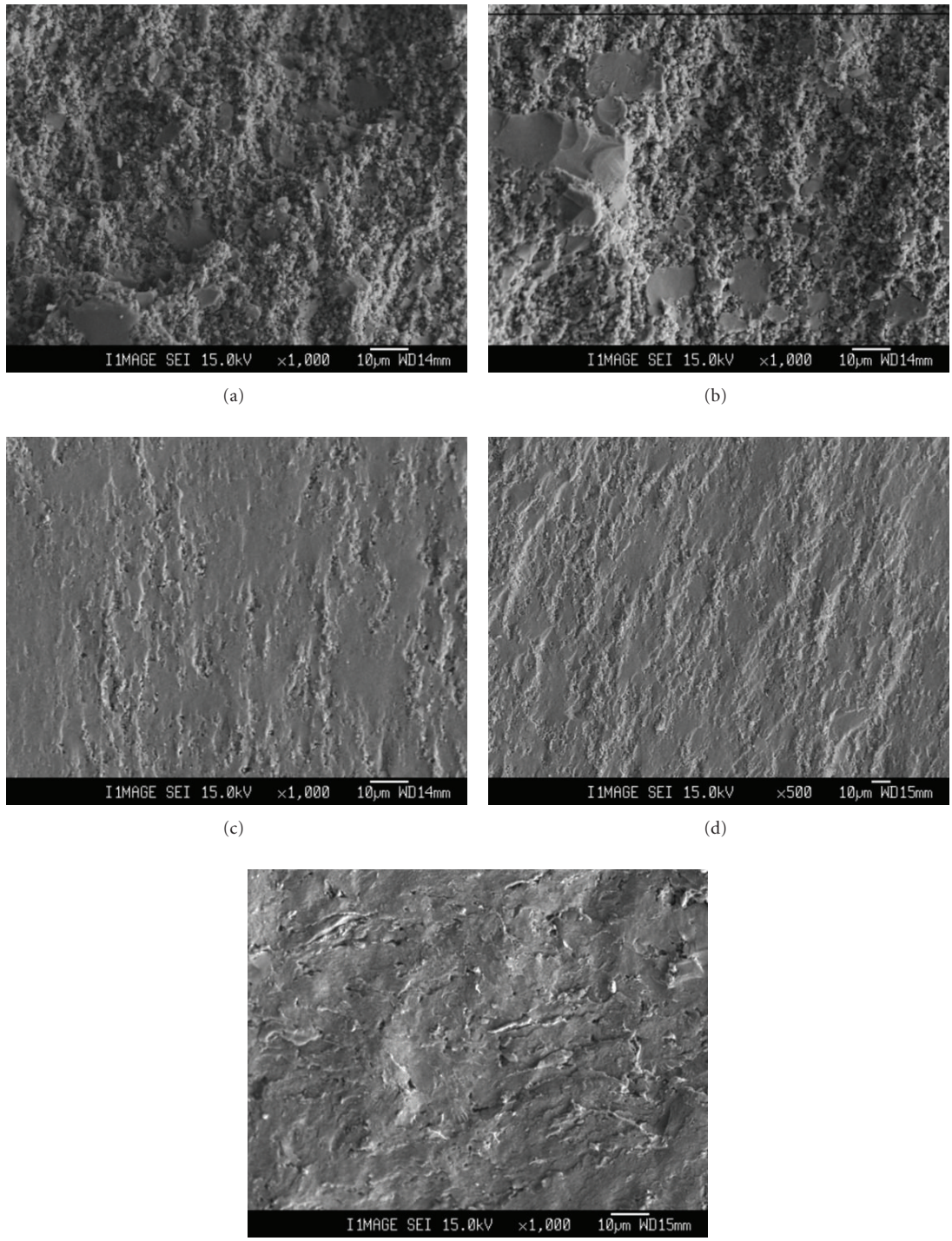

Figure 9: Fracture surface photographs of samples hot pressed under (a) 200 MPa, (b) 300 MPa, (c) 400 MPa, (d) 500 MPa, and (e) 600 MPa pressure at a constant temperature 550°C.

does not remain after consolidation at temperature of 550°C for 30 min. The presence of the crystalline phase in the amorphous matrix in the consolidated bulk sample can be further confirmed by TEM and elemental maps. The TEM micrograph and elemental map of the hot-pressed sample are shown in Figures 12 and 13, respectively, where limited nanocrystallization (formation of AlTi with average size of 10 nm in the amorphous matrix) occurred during

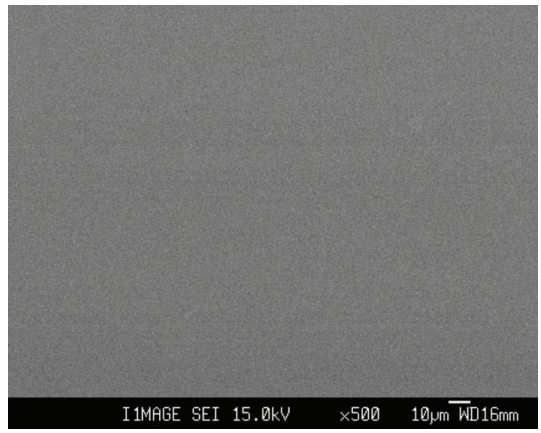

Figure 10: Polished cross-sectional view of sample hot pressed at 550°C under 600 MPa.

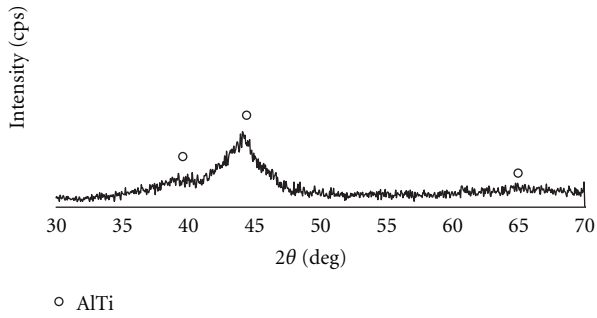

Figure 11: XRD pattern of sample hot pressed at 550°C under 600 MPa.

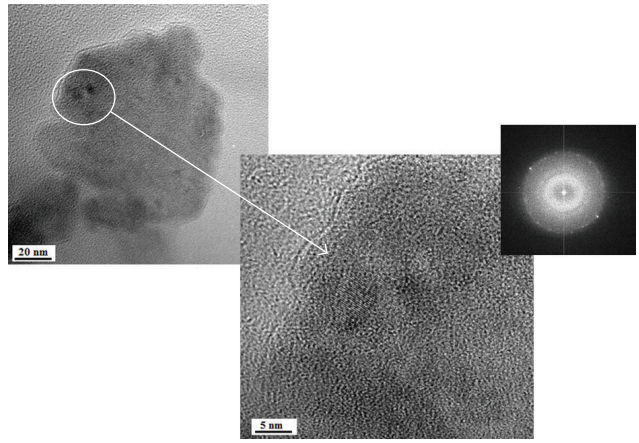

Figure 12: TEM image of sample hot pressed at 550°C under 600 MPa.

the consolidation processes and the produced bulk material is not fully amorphous.

3.4. Thermal Behavior of Produced Bulk Material. In order to investigate the thermal behavior and microstructural changes of the consolidated bulk amorphous alloy (below crystallization temperature), pressed samples were annealed at several temperatures for 3 h. XRD patterns of as-hot pressed and annealed samples at 550°C, 600°C, 650°C, and 700°C are presented in Figure 14. During the consolidation of the amorphous powders at 550°C for 30 min, the AlTi phase precipitates in the amorphous matrix. Analysis of the XRD patterns in Figure 14 reveals that by annealing the samples at temperature above 550°C (below crystallization temperature), the AlTi diffraction peaks disappeared and several peaks corresponding to $Al_{13}(Fe,Ni)_4$ and Al_3Ti intermetallic

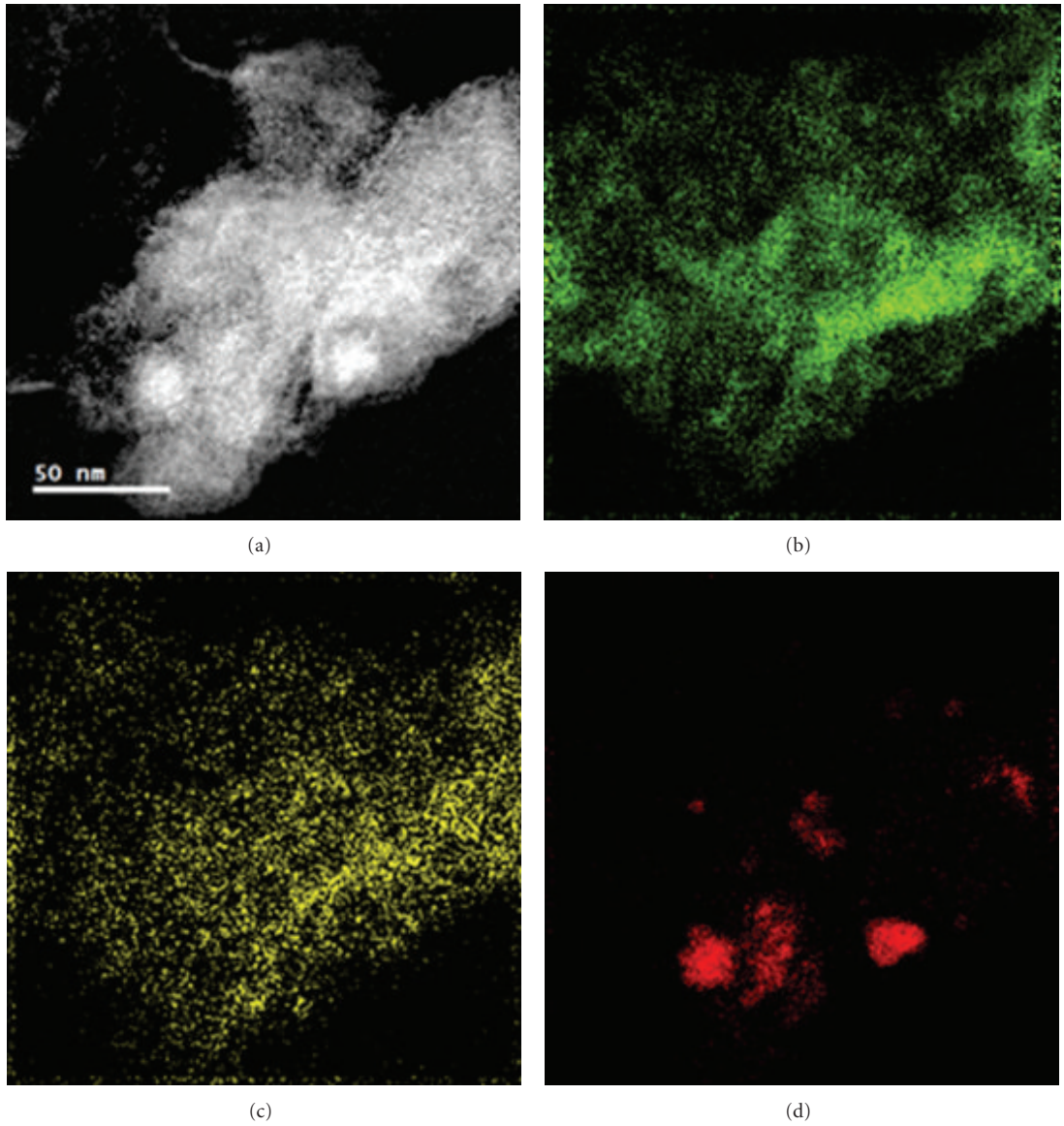

Figure 13: (a) Al, (b) Ni, (c) Fe, and (d) Ti elemental maps of the sample hot pressed at 550°C under 600 MPa.

phases appeared. By increasing the annealing temperature, the intensity of $Al_{13}(Fe,Ni)_4$ and Al_3Ti peaks in the XRD patterns increases as a result of increasing the crystalline size and the fraction of this phase during annealing.

4. Conclusions

In the present work, we fabricated amorphous $Al_{80}Fe_{10}Ti_5Ni_5$ powders by milling elemental powder mixtures for 40 h. The crystallization process of this amorphous alloy is a one-stage mode of the $Al_{13}(Fe,Ti)_4$ and Al_3Ti intermetallic compounds. The results showed that the as-milled amorphous $Al_{80}Fe_{10}Ti_5Ni_5$ powders were consolidated successfully into bulk metallic glasses by a hot pressing technique. The temperature and pressure for successful condensation of amorphous powders in the hot

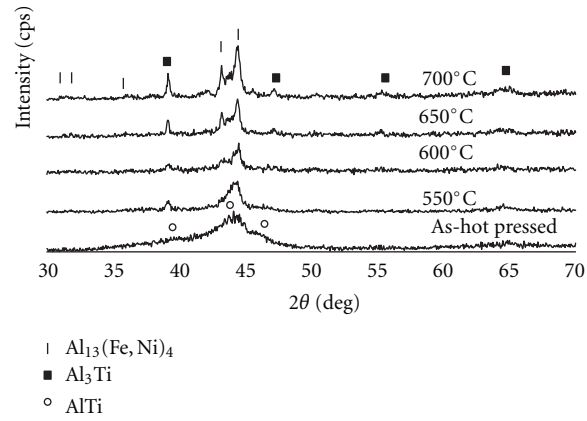

Figure 14: XRD patterns of samples as-hot pressed and annealed at 550°C, 600°C, 650°C, and 700°C for 3 h.

pressing method are 550°C and 600 MPa, respectively. During the consolidation, the amorphous phase does not remain and an AlTi intermetallic phase precipitates in the amorphous matrix.

Acknowledgments

This work was supported by the National Research Foundation of Korea (NRF) grant funded by the Korea government (MEST, no. 2010-0026981). H. S. Kim acknowledges the support of a grant (B551179-08-01-00) from the cooperative research project "Development of common manufacturing technology for high functional susceptor" funded by the Ministry of Knowledge Economy, Republic of Korea.

References

[1] H. S. Kim, P. J. Warren, B. Cantor, and H. R. Lee, "Mechanical properties of partially crystallized aluminum based amorphous alloys," *Nanostructured Materials*, vol. 11, no. 2, pp. 241–247, 1999.

[2] H. S. Kim and S. I. Hong, "A model of the ductile-brittle transition of partially crystallized amorphous Al-Ni-Y alloys," *Acta Materialia*, vol. 47, no. 7, pp. 2059–2066, 1999.

[3] H. S. Kim, "Yield and compaction behavior of rapidly solidified Al-Si alloy powders," *Materials Science and Engineering A*, vol. 251, no. 1-2, pp. 100–105, 1998.

[4] H. Asgharzadeh, A. Simchi, and H. S. Kim, "Hot deformation of ultrafine-grained Al6063/Al_2O_3 nanocomposites," *Journal of Materials Science*, vol. 46, no. 14, pp. 4994–5001, 2011.

[5] S.-H. Lee and C.-S. Kang, "Fabrication and estimation of an ultrafine grained complex aluminum alloy sheet by the ARB process using dissimilar aluminum alloys," *Journal of Korean Institute of Metals and Materials*, vol. 49, no. 11, pp. 893–899, 2011.

[6] W.-D. Kang and H. G. Park, "Influence of Zr addition on TiB2 modification and grain size in aluminium alloys," *Journal of Korean Institute of Metals and Materials*, vol. 49, pp. 619–627, 2011.

[7] K. J. Lee and K. D. Woo, "Effect of pre-aging conditions on bake-hardening response of Al-0.4 wt%Mg-1.2 wt%Si-0.1 wt%Mn alloy sheets," *Journal of Korean Institute of Metals and Materials*, vol. 49, no. 6, pp. 448–453, 2011.

[8] F. Cardellini, V. Contini, R. Gupta et al., "Microstructural evolution of Al-Fe powder mixtures during high-energy ball milling," *Journal of Materials Science*, vol. 33, no. 10, pp. 2519–2527, 1998.

[9] H. S. Kin, S. J. Kim, H. R. Lee, C. W. Won, S. S. Cho, and B. S. Chun, "Compaction behavior of rapidly solidified Al-Si-Fe-Cr alloy powders," *Scripta Materialia*, vol. 37, no. 11, pp. 1715–1719, 1997.

[10] M. Krasnowski, A. Grabias, and T. Kulik, "Phase transformations during mechanical alloying of Fe-50% Al and subsequent heating of the milling product," *Journal of Alloys and Compounds*, vol. 424, no. 1-2, pp. 119–127, 2006.

[11] M. Tavoosi, M. H. Enayati, and F. Karimzadeh, "Crystallisation process of $Al_{80}Fe_{10}Ti_{10}$ amorphous phase," *Powder Metallurgy*, vol. 54, no. 3, pp. 445–449, 2011.

[12] M. Tavoosi, F. Karimzadeh, M. H. Enayati, S. H. Joo, and H. S. Kim, "Amorphous phase formation in $Al_{80}Fe_{10}M_{10}$ (M = Ni, Ti, and V) ternary systems by mechanical alloying," *Journal of Materials Science*, vol. 46, no. 23, pp. 7633–7638, 2011.

[13] A. Inoue, "Amorphous, nanoquasicrystalline and nanocrystalline alloys in Al-based systems," *Progress in Materials Science*, vol. 43, no. 5, pp. 365–520, 1998.

[14] S. J. Hong, T. S. Kim, H. S. Kim, W. T. Kim, and B. S. Chun, "Microstructural behavior of rapidly solidified and extruded Al-14wt%Ni-14wt%Mm (Mm, Misch metal) alloy powders," *Materials Science and Engineering A*, vol. 271, no. 1-2, pp. 469–476, 1999.

[15] S.-C. Park, M.-S. Kim, K.-T. Kim, S.-Y. Shin, J.-K. Lee, and K.-H. Ryu, "Compressive deformation behavior of Al-10Si-5Fe-1Zr powder alloys consolidated by spark plasma sintering process," *Journal of the Korean Institute of Metals and Materials*, vol. 49, pp. 853–859, 2011.

[16] C. S. Han and S. O. Han, "A study on the fabrication and structural properties of Al-Co/AlN-Co thin films," *Journal of Korean Institute of Metals and Materials*, vol. 49, no. 3, pp. 256–263, 2011.

[17] I.-H. Kim, B.-S. Chun, and S.-J. Hong, "The effects of electron beam irradiation direction on mechanical properties and microstructural characteristics of thick Al 5052 alloy plate," *Metals and Materials International*, vol. 17, no. 2, pp. 357–363, 2011.

[18] D.-H. Ahn, H. S. Kim, and Y. Estrin, "A semi-phenomenological constitutive model for hcp materials as exemplified by alpha titanium," *Scripta Materialia*, vol. 67, no. 2, pp. 121–124, 2012.

[19] H. S. Kim, "Hardening behaviour of partially crystallised amorphous Al alloys," *Materials Science and Engineering A*, vol. 304-306, no. 1-2, pp. 327–331, 2001.

[20] H. Gleiter, "Materials with ultrafine microstructures: retrospectives and perspectives," *Nanostructured Materials*, vol. 1, no. 1, pp. 1–19, 1992.

[21] G. W. Nieman, J. R. Weertman, and R. W. Siegel, "Mechanical behavior of nanocrystalline metals," *Nanostructured Materials*, vol. 1, no. 2, pp. 185–190, 1992.

[22] C. Suryanarayana, "Mechanical alloying and milling," *Progress in Materials Science*, vol. 46, no. 1-2, pp. 1–184, 2001.

[23] F. Zhou, R. Lück, M. Scheffer, D. Lang, and K. Lu, "The crystallization process of amorphous $Al_{80}Fe_{20}$ alloy powders prepared by ball milling," *Journal of Non-Crystalline Solids*, vol. 250–252, pp. 704–708, 1999.

[24] Y. B. Kim, H. M. Park, W. Y. Jeung, and J. S. Bae, "Vacuum hot pressing of gas-atomized Ni-Zr-Ti-Si-Sn amorphous powder," *Materials Science and Engineering A*, vol. 368, no. 1-2, pp. 318–322, 2004.

[25] K. Hanada, Y. Murakoshi, H. Negishi, and T. Sano, "Microstructures and mechanical properties of Al-Li/SiCp composite produced by extrusion processing," *Journal of Materials Processing Technology*, vol. 63, no. 1–3, pp. 405–410, 1997.

[26] M. J. Tan and X. Zhang, "Powder metal matrix composites: selection and processing," *Materials Science and Engineering A*, vol. 244, no. 1, pp. 80–85, 1998.

[27] H. S. Kim and D. N. Lee, "Power-law creep model for densification of powder compacts," *Materials Science and Engineering A*, vol. 271, no. 1-2, pp. 424–429, 1999.

[28] S. C. Yoon, S. J. Hong, S. I. Hong, and H. S. Kim, "Mechanical properties of equal channel angular pressed powder extrudates of a rapidly solidified hypereutectic Al-20 wt% Si alloy," *Materials Science and Engineering A*, vol. 449–451, pp. 966–970, 2007.

[29] A. Saleh, S. Heshmati-Manesh, S. Sheibani, and A. Ataie, "Consolidation of nano-crystalline copper powder by cold and

hot pressing," *Metals and Materials International*, vol. 17, no. 5, pp. 749–753, 2011.

[30] H. Kwon, M. Leparoux, J.-M. Heintz, J.-F. Silvain, and A. Kawasaki, "Fabrication of single crystalline diamond reinforced aluminum matrix composite by powder metallurgy route," *Metals and Materials International*, vol. 17, no. 5, pp. 755–763, 2011.

[31] JCPDS 50-0797, International Centre for Diffraction Data, 2012.

[32] JCPDS 14-0451, International Centre for Diffraction Data, 2012.